INTERNATIONAL JOURNAL FOR NUMERICAL METHODS IN FLUIDS
Int. J. Numer. Meth. Fluids **30**: 233–256 (1999)

A NUMERICAL STUDY OF PROJECTION ALGORITHMS IN THE FINITE ELEMENT SIMULATION OF THREE-DIMENSIONAL VISCOUS INCOMPRESSIBLE FLOW

Dedicated to Roland Glowiski on the occasion of his sixtieth birthday.

D. GOLDBERG[1] AND V. RUAS*,[2]

Laboratoire de Modélisation en Mécanique, Université Pierre et Marie Curie, 75252, Paris Cedex 05, France

SUMMARY

In this work a comparative study of two versions of the projection algorithm used either for time integration or as an iterative method to solve the three-dimensional incompressible Navier–Stokes equations is presented. It is also shown that these projection algorithms combined with the finite element method are particularly suited for the treatment of outflow boundary conditions in the context of external flows. This assertion is illustrated by means of some numerical examples in which five types of boundary conditions are compared. The scheme is applied to simulate the flow past a cylinder clamped on two fixed parallel solid walls. Comparison with experimental data available for this problem shows good agreement of the velocity and pressure fields, both computed with continuous piecewise linear elements. Copyright © 1999 John Wiley & Sons, Ltd.

KEY WORDS: projection method; finite element; 3D flow; Bi-CGSTAB

1. NOTATIONS

The sets involved in the equations considered hereafter are classical spaces of functions defined in the flow domain $\Omega \subset \mathbb{R}^3$ with boundary $\partial\Omega$, whose definitions are recalled below:

$$L^2(\Omega) = \left\{ q / \int_\Omega q^2 < \infty \right\}; \qquad L^2_0(\Omega) = \left\{ q / q \in L^2(\Omega) \text{ and } \int_\Omega q = 0 \right\}$$

$$H^1(\Omega) = \{ q / |\nabla q| \in L^2(\Omega) \}; \qquad H^1_0(\Omega) = \{ q / q \in H^1(\Omega) \text{ and } q = 0 \text{ on } \partial\Omega \}.$$

* Correspondence to: Laboratoire de Modélisation en Mécanique, CNRS URA No. 229, Université Pierre et Marie Curie, Boite 162, 4 Place Jussîeu, 75252, Paris Cedex 05, France.
[1] Current address: Département de Mathématiques, Université Paris 8, France.
[2] Current address: Université de Saint Etienne, France.

CCC 0271–2091/99/110233–24$17.50

Received September 1996
Revised November 1997

2. INTRODUCTION

In the framework of the numerical solutions of the incompressible Navier–Stokes equations there are a few iteration techniques or time integration schemes widely used, which linearize the problem to be solved at every step. Among these, fractional step algorithms that transform the problem at every such stage of the solution procedure into a sequence of problems, including Stokes systems, have proven to be quite effective.

For early versions of this methodology, the authors refer to Bristeau *et al.* [1], while quoting some recent variants of it in connection with the fictitious domain technique (Glowinski [2]).

Another approach intensely exploited by some authors is the fully explicit solution scheme for computing the velocity at every step, followed by the determination of the pressure through the solution of a Poisson equation. For details on this method the authors refer to Shimura and Kawahara [3].

Since the early 1960s, the idea of splitting the problem at every step into the calculation of a non- (necessarily) solenoidal velocity field, by solving an uncoupled advection–diffusion system, followed by a correction step in which a solenoidal velocity and the pressure are both derived from the above, appeared to be attractive to many specialists. Actually, this approach commonly called the projection method, widely in use since then, in the context of finite difference space discretizations, has the main advantage of allowing the uncoupled computation of the velocity and the pressure.

For this reason, like several others (see e.g. Heywood *et al.* [4]), the authors developed projection methods combined with a finite element discretization, as it naturally leads to the consideration of different possible variational forms, besides a number of other relevant theoretical and practical issues.

Incidentally, a rather recent survey of finite element techniques used for solving three-dimensional incompressible flows can be found in Ruas [5], supplemented by Ruas *et al.* [6] and references therein.

As a matter of fact, the numerical approach used here is based on the following choices. First, the split treatment of the Navier–Stokes equations is performed by means of two types of projection methods, precisely, the original Chorin–Temam one [7,8] and a modification of it due to Goda [9]. A post-processing of the pressure allows the lack of accuracy usually encountered in that type of method to be circumvented.

Actually, the authors show that this operation can be performed quite easily and naturally in a variational context. In so doing, they show that the finite element method presents an additional advantage when chosen as a discretization method applied to the equations derived from projection algorithms. Moreover, as it is well-known for almost two decades, the variational approach lends itself naturally to stabilization techniques of the streamline–diffusion type, such as the streamline-upwind Petrov–Galerkin (SUPG) (Brooks and Hughes [10]), for an efficient treatment of high Reynolds number flows. In this paper, the authors use a particular variant of it described in Section 3.

It is shown through an *a priori* analysis confirmed by a series of numerical examples with known analytical solutions that classical piecewise linear finite elements are reliable and accurate in the particular versions of projection algorithms in use. The ability of these algorithms to effectively produce stationary solutions is also analysed.

The non-symmetric linear systems involved in the advection–diffusion step of the projection algorithm are solved by an improvement of the conjugate gradient method, named Bi-CGSTAB (for biconjugate gradient with stabilization [11]). This one is preconditioned by an incomplete factorization leading to a matrix that shows the same sparse structure as the system matrix.

In this respect, the authors point out an additional merit of the SUPG stabilization. Indeed, one of its main effects is to add a symmetric positive semi-definite part to the discretization matrix corresponding to the standard Galerkin formulation of the advection–diffusion equation, without endangering qualitative approximation properties. Hence, they reduce significantly the risk of incomplete factorization breakdowns, which often happen to Navier–Stokes equations discretization matrices. Actually, this did not occur in any of the present numerical experiments.

Additionally, within the aim of reducing storage requirements, the conjugate gradient method with incomplete Cholesky factorization pre-conditioning is also used in this paper to solve all the linear systems of equations with a symmetric positive definite matrix.

The choice of the model problem, i.e. the flow past a cylinder, allows comparisons between experimental and other numerical results. It also allows the comparison and validation or not of several types of outflow boundary conditions specified in Section 4, to be used in connection with projection algorithms. Some of the validated conditions were recently used by other authors too (see [4]). An extensive study on outflow boundary conditions in the context of two-dimensional flows can be found in Sani and Gresho [12].

3. THE PROJECTION ALGORITHMS AND THEIR VARIATIONAL FORMS

The authors consider the incompressible Navier–Stokes equations: find a velocity field u and a pressure p in a flow domain Ω, such that for given body forces f the following system holds:

$$\begin{cases} \dfrac{\partial u}{\partial t} - \dfrac{1}{Re}\,\Delta u + (u\cdot\nabla)u + \nabla p = f \\ \nabla\cdot u = 0 \end{cases}, \tag{1}$$

where Re is the Reynolds number, with suitable conditions on the boundary of the domain, and a given velocity u_0 at time $t=0$.

For a given time step Δt and setting $u^0 = u_0$, a semi-implicit time discretization of (1) consists of approximating $u(\,.\,, n\Delta t)$ and $p(\,.\,, n\Delta t)$ for $n = 1, 2, \ldots$ by the solution (u^n, p^n) of:

$$\begin{cases} \dfrac{u^n - u^{n-1}}{\Delta t} - \dfrac{1}{Re}\,\Delta u^n + (u^{n-1}\cdot\nabla)u^n + \nabla p^n = f \\ \nabla\cdot u^n = 0 \end{cases} \tag{2}$$

with boundary conditions derived from those of system (1).

The aim of the projection methods is to decompose the former system into two steps, namely, an advection–diffusion one and a projection one. The main advantage thus obtained is the uncoupled computation of the velocity and the pressure. The algorithm (in its original formulation) is written as follows:

u^0 given.
For $n = 1, 2, \ldots,$ compute u^n and p^n_* by:

$$\begin{cases} \dfrac{u^n - u^n_*}{\Delta t} + \nabla p^n_* = 0 \\ \nabla \cdot u^n = 0 \end{cases}, \tag{3}$$

where u^n_* is the solution of:

$$\frac{u^n_* - u^{n-1}}{\Delta t} - \frac{1}{Re}\Delta u^n_* + (u^{n-1}\cdot\nabla)u^n_* = f \tag{4}$$

with corresponding boundary conditions.

The combination of the two equations of (3) gives:

$$\Delta p^n_* = \frac{\nabla \cdot u^n_*}{\Delta t}. \tag{5}$$

Assuming that $(u^n - u^n_*)\cdot \vec{v} = 0$ on $\partial\Omega$, the Neumann boundary condition $\partial p^n_*/\partial v = 0$ applies, where $\vec{v}$ denotes the unit outer normal vector on $\partial\Omega$.

In fact, even if u^n is a good approximation of u, in general p^n_* does not approximate very well the physical pressure p. For this reason the authors use a post-processing of it, which consists of computing the final pressure from the velocity u^n by

$$\Delta p^n = \nabla \cdot f - \nabla \cdot [(u^n \cdot \nabla)u^n]. \tag{6}$$

In fact, the underlying boundary condition:

$$\frac{\partial p^n}{\partial v} = -[(u^n\cdot\nabla)u^n]\cdot\vec{v} + \frac{1}{Re}\Delta u^n \cdot \vec{v} \tag{7}$$

can be simplified for sufficiently high Reynolds numbers into:

$$\frac{\partial p^n}{\partial v} = -[(u^n\cdot\nabla)u^n]\cdot\vec{v}. \tag{8}$$

Summarizing in the case where velocity boundary conditions of the Dirichlet type are prescribed on $\partial\Omega$, the variational form of the two selected algorithms is:

$$\int_\Omega \frac{(u^n_* - u^{n-1})\cdot v}{\Delta t} + \frac{1}{Re}\int_\Omega \nabla u^n_* \cdot \nabla v + \int_\Omega (u^{n-1}\cdot\nabla)u^n_* \cdot v = \int_\Omega f\cdot v - \int_\Omega \nabla \tilde{p}^{n-1}\cdot v \quad \forall v \in (H^1_0(\Omega))^3, \tag{9}$$

$$\int_\Omega \nabla p^n_* \cdot \nabla q = -\int_\Omega \frac{\nabla \cdot u^n_*}{\Delta t}\cdot q \quad \forall q \in H^1(\Omega)\cap L^2_0(\Omega), \tag{10}$$

$$\int_\Omega u^n \cdot v = \int_\Omega u^n_* \cdot v - \Delta t \int_\Omega \nabla p^n_* \cdot v \quad \forall v \in (H^1_0(\Omega))^3, \tag{11}$$

$$\int_\Omega \nabla p^n \cdot \nabla q = \int_\Omega f\cdot\nabla q - \int_\Omega \nabla\cdot[(u^{n-1}\cdot\nabla)u^n]\cdot\nabla q \quad \forall q \in H^1(\Omega)\cap L^2_0(\Omega), \tag{12}$$

with suitable boundary data for both u^n_* and u^n.

The value of $\tilde{p}^n$ determines which projection algorithm is being used. This is defined as follows:

$\tilde{p}^0 = 0$

- 1st algorithm (the Chorin–Temam scheme): $\tilde{p}^n = \tilde{p}^{n-1} \quad \forall n,$ (13)
- 2nd algorithm (Goda's scheme): $\tilde{p}^n = \tilde{p}^{n-1} + p^n_* \quad \forall n.$ (14)

In order to stabilize the discrete version of problem (9) when Re is large, the authors use a modified version of this variational form obtained by replacing the test function v with:

$$v + \rho(u^{n-1} \cdot \nabla)v$$

in all terms involved except the one preceded by $1/Re$. Indeed, this term gives no contribution owing to the choice of the finite elements in use. ρ is a parameter depending on the average edge lengths of the elements, which is adjusted in a manner adapted from the techniques studied in Franca and Frey [13], Behr *et al.* [14] and Franca and Hughes [15]. More specifically, ρ is the following constant over each tetrahedron K of the mesh:

$$\rho/K = \frac{h_K}{2|\vec{u}^{n-1}(G_K)|},$$

where h_K is the averaged edge length of K and G_K is the barycenter of K.

The fact that no correction of this value is taken for small element Reynolds numbers is justified by the fact that the computations are three-dimensional, which prevents producing values of h_K too small. Moreover, in most of the tests performed, the Reynolds number is sufficiently large to prevent any element Reynolds number from being less than 1. Finally, in all the cases considered, the computations validated this simplified choice of the stabilization parameter ρ, which incidentally avoid the complex calculation of inverse inequality constants (cf. Franca and Frey [13]). For other choices of ρ that have proven to work well, the authors refer to Tezduyar *et al.* [16] or Tezduyar *et al.* [17].

Finally, an analysis restricted to a linearized step indicates (see [18]) that piecewise linear finite elements appear to be an ideal choice to carry out the discretization of the problem unknowns, even with a non-optimal choice of Δt related to the mesh step size. This point is developed Section 5.

4. DESCRIPTION OF THE MODEL PROBLEM

A code was developed using the above described methodology in order to solve time-dependent problems. Here it was tested in the framework of the early stages of the classical flow past a cylinder at different Reynolds numbers and for $f = 0$. The domain Ω is defined as

$$\Omega = \{(x, y, z) \in \mathbb{R}^3 / -5 \le x \le 10, \ -5 \le y \le 5, \ 0 \le z \le Z, \ x^2 + y^2 \ge 1\}.$$

Two cylinder lengths were tested: $Z = 5$ and 10. The boundary conditions are:

$$u = \begin{cases} (0, 0, 0) \text{ for } x^2 + y^2 = 1, \ z = 0 \text{ and } z = Z, \\ (\underline{u}, 0, 0) \text{ for } x = -5 \text{ and for } y = \pm 5 \text{ provided } z \neq 0 \text{ and } z \neq Z, \end{cases}$$

where $\mathbf{u} = 4z(Z - z)$ or $\mathbf{u} = 1$.

Furthermore, some outflow boundary conditions involving the velocity, the pressure and/or the vorticity have been studied (on $x = 10$):

(A) $$\frac{\partial u_x}{\partial x} = u_y = u_z = p = 0,$$

(B) $\dfrac{\partial \omega_x}{\partial x} = \omega_z = p = 0 \quad \text{and} \quad \omega_y = \dfrac{\partial \underline{u}}{\partial z}$,

(C) $\dfrac{\partial u_y}{\partial x} = \dfrac{\partial u_z}{\partial x} = 0, \qquad u_x = \underline{u}_x \quad \text{and} \quad \dfrac{\partial p}{\partial x} = 0,$

(D) $\omega_z = p = 0$, and other undefined conditions on u or ω,

where $\omega = \nabla \wedge u$ is the vorticity and u is the given inflow velocity.

Remark 1: These conditions may be implemented by prescribing the following conditions on u_*^n and p_*^n:

C.L. 1 $\dfrac{\partial u_{*x}^n}{\partial x} = u_{*y}^n = u_{*z}^n = p_*^n = 0, \qquad \Rightarrow$(A)

C.L. 2 $u_{*x}^n = \underline{u}_x, \qquad u_{*y}^n = u_{*z}^n = p_*^n = 0, \qquad \Rightarrow$(A)

C.L. 3 $\dfrac{\partial u_{*x}^n}{\partial x} = \dfrac{\partial u_{*z}^n}{\partial x} = p_*^n = 0 \quad \text{and} \quad \dfrac{\partial u_{*y}^n}{\partial x} = \dfrac{\partial u_{*x}^n}{\partial y}, \qquad \Rightarrow$(D)

C.L. 4 $u_{*x}^n = \underline{u}_x, \qquad \dfrac{\partial u_{*y}^n}{\partial x} = \dfrac{\partial u_{*z}^n}{\partial x} = p_*^n = 0, \qquad \Rightarrow$(B)

C.L. 5 $u_{*x}^n = \underline{u}_x, \qquad \dfrac{\partial u_{*y}^n}{\partial x} = \dfrac{\partial u_{*z}^n}{\partial x} = \dfrac{\partial p_*^n}{\partial x} = 0, \qquad \Rightarrow$(C)

After several tests (see Section 6.2), the authors concluded that the most interesting compromise cost realism is obtained through the use of condition C.L. 1. In this respect, assuming sufficient smoothness of p_*^n, it is noted that on the outflow boundary $x = \text{constant}$, one has:

$$\frac{\partial u_x^n}{\partial x} = \frac{\partial u_{*x}^n}{\partial x} - \Delta t \frac{\partial^2 p_*^n}{\partial x^2} = -\Delta t \frac{\partial^2 p_*^n}{\partial x^2} = -\Delta t \Delta p_*^n = -\nabla \cdot u_*^n.$$

Since $\nabla \cdot u_*^n = \partial u_{*x}^n / \partial x = 0$ by assumption, one has $\partial u_x^n / \partial x = 0$.

Moreover, one also has $u_y^n = u_{*y}^n - \Delta t \, (\partial p_*^n / \partial y) = 0$ (respectively $u_z^n = 0$) on the outflow boundary.

5. STUDY OF THE SPACE DISCRETIZATION

In order to derive conditions indicating the adequacy of the finite elements discretization in use in connection with (3)–(5) and on the appropriate choice of parameter Δt, the authors perform the following *a priori* estimate restricted to a given time step for the underlying Stokes problem:

$$\frac{u_*^n - u^{n-1}}{\Delta t} - \frac{1}{Re} \Delta u_*^n = f, \tag{15}$$

$$\Delta p_*^n = \frac{\nabla \cdot u_*^n}{\Delta t}, \tag{16}$$

$$u^n = u_*^n - \Delta t \nabla p_*^n. \tag{17}$$

The variational form of this system is:

$$\int_\Omega u_*^n \cdot v_* + \frac{\Delta t}{Re} \int_\Omega \nabla u_*^n \cdot \nabla v_* = \Delta t \int_\Omega f \cdot v_* - \int_\Omega u^{n-1} \cdot v_* \quad \forall v_* \in (H_0^1(\Omega))^3, \tag{18}$$

$$\Delta t \int_\Omega \nabla p_*^n \cdot \nabla q = \int_\Omega u_*^n \cdot \nabla q \quad \forall q \in L_0^2(\Omega)/\mathbb{R}, \tag{19}$$

$$\int_\Omega u^n \cdot v = \int_\Omega u_*^n \cdot v - \Delta t \int_\Omega \nabla p_*^n \cdot v \quad \forall v \in (H_0^1(\Omega))^3. \tag{20}$$

In order to study the convergence of system (18)–(20) in a least-squares sense, the authors consider the underlying bilinear form:

$$\begin{aligned} &a((u, u_*, p_*), (v, v_*, q)) \\ &= \frac{1}{\Delta t} \int_\Omega u_* \cdot v_* + \frac{1}{Re} \int_\Omega \nabla u_* \cdot \nabla v_* + \Delta t \int_\Omega \nabla p_* \cdot \nabla q - \int_\Omega u_* \cdot \nabla q + \int_\Omega u \cdot v - \int_\Omega u_* \cdot v \\ &\quad + \Delta t \int_\Omega \nabla p_* \cdot v \end{aligned}$$

and norm:

$$|||(v, v_*, q)||| = \left(\frac{1}{\Delta t} \|v_*\|^2 + \frac{1}{Re} \|\nabla v_*\|^2 + \Delta t \|\nabla q\|^2 + \|v\|^2 \right)^{1/2},$$

where $\| \ \|$ is the classical norm on L^2.

The coerciveness of a is derived for $\Delta t \leq 1/4$ by:

$$\begin{aligned} &a((v, v_*, q), (v, v_*, q)) \\ &= \frac{1}{\Delta t} \|v_*\|^2 + \frac{1}{Re} \|\nabla v_*\|^2 + \Delta t \|\nabla q\|^2 - \int_\Omega v_* \cdot \nabla q + \|v\|^2 - \int_\Omega v_* \cdot v - \Delta t \int_\Omega \nabla q \cdot v \\ &\geq \frac{1}{\Delta t} \|v_*\|^2 + \frac{1}{Re} \|\nabla v_*\|^2 + \Delta t \|\nabla q\|^2 - \frac{1}{2} \left(\Delta t \|\nabla q\|^2 + \frac{1}{\Delta t} \|v_*\|^2 \right) + \|v\|^2 - \frac{1}{2} (\|v\|^2 + \|v_*\|^2) \\ &\quad - \Delta t \left(\frac{\|\nabla q\|^2}{4} + \|v\|^2 \right) \\ &\geq \frac{1}{2} \left(\frac{1}{\Delta t} - 1 \right) \|v_*\|^2 + \frac{1}{Re} \|\nabla v_*\|^2 + \frac{\Delta t}{4} \|\nabla q\|^2 + \left(\frac{1}{2} - \Delta t \right) \|v\|^2 \\ &\geq \frac{3}{2\Delta t} \|v_*\|^2 + \frac{1}{Re} \|\nabla v_*\|^2 + \frac{\Delta t}{4} \|\nabla q\|^2 + \frac{1}{4} \|v\|^2 \quad \text{for} \quad \Delta t \leq 1/4 \\ &\geq \frac{1}{4} |||(v, v_*, q)|||^2. \end{aligned}$$

The coerciveness is so proved with the constant $\alpha = 1/4$.

Furthermore,

$$\begin{aligned} &a((u, u_*, p_*), (v, v_*, q)) \\ &\leq \frac{1}{\Delta t} \|u_*\| \|v_*\| + \frac{1}{Re} \|\nabla u_*\| \|\nabla v_*\| + \Delta t \|\nabla p_*\| \|\nabla q\| + \|u_*\| \|\nabla q\| + \|u\| \|v\| + \|u_*\| \|v\| \\ &\quad + \Delta t \|\nabla p_*\| \|v\| \end{aligned}$$

$$\leq \left(\frac{1}{\Delta t} \|u_*\| \|v_*\| + \frac{1}{Re} \|\nabla u_*\| \|\nabla v_*\| + \Delta t \|\nabla p_*\| \|\nabla q\| + \|u\| \|v\| \right)$$
$$+ \left(\|u_*\| \|\nabla q\| + \frac{1}{\sqrt{\Delta t}} \|u_*\| \|v\| + \sqrt{\Delta t} \int_\Omega \nabla p_* \cdot v \right) \quad \text{for} \quad \Delta t < 1.$$

Each term of the right-hand-side above is less or equal to:

$$\sqrt{2} \left(\frac{\|u_*\|^2}{\Delta t} + \frac{\|\nabla u_*\|^2}{Re} + \Delta t \|\nabla p_*\|^2 + \|u\|^2 \right)^{1/2} \times \left(\frac{\|v_*\|^2}{\Delta t} + \frac{\|\nabla v_*\|^2}{Re} + \Delta t \|\nabla q\|^2 + \|v\|^2 \right)^{1/2}.$$

Then, the continuity of the form a is obtained for $\Delta t < 1$:

$$a((u, u_*, p_*), (v, v_*, q)) \leq M |||(u, u_*, p_*)||| \, |||(v, v_*, q)||| \quad \text{with} \quad M = 2\sqrt{2}\,.$$

The Lax–Milgram theorem allows the conclusion of the existence and the uniqueness of the solution and Céa's lemma leads to the study of the error bound:

$$|||(u - u^h, u_* - u_*^h, p_* - p_*^h)||| \leq \frac{M}{\alpha} \inf_{\substack{(v, v_*) \in V_h^2 \\ q \in Q_h}} |||(u - v, u_* - v_*, p_* - q)|||,$$

where (u^h, u_*^h), p_*^h are the approximations of (u, u_*), p_* obtained with the underlying finite element method, namely the one associated with the spaces V_h and Q_h of continuous piecewise linear vector fields or functions in the usual manner. A straightforward calculation yields:

$$|||(u - u^h, u_* - u_*^h, p_* - p_*^h)|||$$
$$\leq 8\sqrt{2} \inf_{\substack{(v, v_*) \in V_h^2 \\ q \in Q_h}} \left(\frac{1}{\Delta t} \|u_* - v_*\|^2 + \frac{1}{Re} \|\nabla(u_* - v_*)\|^2 + \Delta t \|\nabla(p_* - q)\|^2 + \|u - v\|^2 \right)^{1/2}$$
$$\leq 8\sqrt{2} \inf_{\substack{(v, v_*) \in V_h^2 \\ q \in Q_h}} \left(\frac{1}{\sqrt{\Delta t}} \|u_* - v_*\| + \frac{1}{\sqrt{Re}} \|\nabla(u_* - v_*)\| + \sqrt{\Delta t} \|\nabla(p_* - q)\| + \|u - v\| \right)$$
$$\leq 8\sqrt{2} \left(\inf_{v_* \in V_h} \left(\frac{\|u_* - v_*\|}{\sqrt{\Delta t}} + \frac{\|\nabla(u_* - v_*)\|}{\sqrt{Re}} \right) + \inf_{v \in V_h} \|u - v\| + \inf_{q \in Q_h} \sqrt{\Delta t} \|\nabla(p_* - q)\| \right).$$

This immediately suggests that the best compromise cost accuracy relies upon the choice $\Delta t = O(h)$, even though the error of the computed pressure in H^1-norm is no better than an $O(h^{1/2})$. This justifies the pressure post-processing from a velocity whose error in L^2-norm is an $O(h)$. Moreover, this *a priori* analysis suggests that Δt should not be too small as compared with h. In this case, the pressure error could increase significantly, which may pollute the velocity field as well. A confirmation of this statement can be found in a recent work by Guermond and Quartapelle [19].

6. RESULTS AND DISCUSSION

6.1. Tests with known solutions

In the self-explanatory sets of tables below, namely, Tables I, II, III, IV, V and VI, the authors show a summary of the numerical results for two stationary test problems whose exact

Table I. Results for the elementary test at $\Delta t = 0.05$

Projection	$\|u^n - u_{\text{exa}}\|_{L\infty}$	$\|\tilde{p}^n - p_{\text{exa}}\|_{L2}$	$\|p^n - p_{\text{exa}}\|_{L2}$	n[a]
1	0.08062	0.07202	0.05588	37
2	—	—	—	NCV
2.2	0.02534	0.16370	0.03452	46

[a] Number of iterations for convergence.

Table II. Results for the elementary test at $\Delta t = 0.25$

Projection	$\|u^n - u_{\text{exa}}\|_{L\infty}$	$\|\tilde{p}^n - p_{\text{exa}}\|_{L2}$	$\|p^n - p_{\text{exa}}\|_{L2}$	n[a]
1	0.05099	0.13903	0.03798	29
2	—	—	—	NCV
2.2	0.01513	0.20736	0.03416	56

[a] Number of iterations for convergence.

solutions are known. Convergence is to be understood in the sense that the maximum of $|u^n(x) - u^{n-1}(x)|$ over Ω is less than or equal to 10^{-4}. The expression NCV means either that no clear tendency of fulfilment of such a criterion could be observed after a very large number of iterations, or that the solver Bi-CGSTAB diverges.

The first test is an elementary one where the functions belong to the approximation spaces. The velocity is given on the boundary by:

$$u(x, y, z) = (u_x, u_y, u_z),$$

with

$$u_x(x, y, z) = x + y + z,$$

$$u_y(x, y, z) = x + y + z,$$

$$u_z(x, y, z) = -2(x + y + z).$$

In order to obtain a well-posed problem, the pressure was set to vanish at a given point P. The exact values of the velocities are the functions u_x, u_y, and u_z above. The exact pressure is:

Table III. Results for the elementary test at $\Delta t = 0.0125$

Projection	$\|u^n - u_{\text{exa}}\|_{L\infty}$	$\|\tilde{p}^n - p_{\text{exa}}\|_{L2}$	$\|p^n - p_{\text{exa}}\|_{L2}$	n[a]
1	0.03000	0.025600	0.02308	45
2	—	—	—	NCV
2.2	0.00900	0.18044	0.03946	103

[a] Number of iterations for convergence.

Table IV. Results for the modified Couette flow at $\Delta t = 0.025$

	$\|u^n - u_{\text{exa}}\|_{L\infty}$	$\|\tilde{p}^n - p_{\text{exa}}\|_{L2}$	$\|p^n - p_{\text{exa}}\|_{L2}$	n[a]
Projection 1	0.13252	0.97455	0.08289	232

[a] Number of iterations for convergence.

Table V. Results for the modified Couette flow at $\Delta t = 0.05$

	$\|u^n - u_{\text{exa}}\|_{L^\infty}$	$\|\bar{p}^n - p_{\text{exa}}\|_{L^2}$	$\|p^n - p_{\text{exa}}\|_{L^2}$	n[a]
Projection 1	0.07446	0.50063	0.04449	140

[a] Number of iterations for convergence.

Table VI. Results for the modified Couette flow at $\Delta t = 0.1$

	$\|u^n - u_{\text{exa}}\|_{L^\infty}$	$\|\bar{p}^n - p_{\text{exa}}\|_{L^2}$	$\|p^n - p_{\text{exa}}\|_{L^2}$	n[a]
Projection 1	0.24055	0.39183	0.11263	127

[a] Number of iterations for convergence.

$p(x, y, z) = K - x$, with K chosen so as to fulfill the condition $p(P) = 0$. This solution corresponds to $f = (-1, 0, 0)$.

Take $Re = 100$ and $\rho = 0.05$. Three types of schemes have been implemented, the Chorin–Temam ('Projection 1'), the Goda ('Projection 2') and a modification of the latter in which one does not perform the Petrov–Galerkin stabilization on the pressure term of (9) ('Projection 2.2'). The mesh is uniform and consists of 1331 nodes.

The authors compare the exact pressure with the value $\bar{p}^n$ equal respectively to p_*^n in the case of the Chorin–Temam algorithm and to $\tilde{p}^n$ in the case of the Goda algorithm.

These results confirm that the original Chorin–Temam algorithm reaches the stationary solution more easily than the Goda one. They also justify the modification of the latter. Indeed, the algorithm 'Projection 2.2' reaches the stationary solution, whereas the original Goda does not, and turns out to be more accurate than the Chorin–Temam one. Moreover, in both cases, the post-processing of the pressure shows its efficiency.

It is interesting to point out that, although the finite element spaces in use contain the exact velocity and pressure of this test problem, the algorithm itself fails to represent its solution nearly exactly as required. This point is worth an explanation, for it outspokenly reveals one the most well-known drawbacks of projection algorithms: the poor approximation of the pressure. Indeed, since a homogeneous Neumann boundary condition applies to it in the solution of the Poisson problem (5) for p_*^n, it is not possible to compute an exact (or nearly exact) linear pressure, as long as it does not satisfy such a condition! Of course this indicates that in more complex cases the projection algorithm presents an intrinsic default, as far as standard pressure calculations are concerned, and this justifies the need of post-processing this field.

The second test is a modified Couette flow (Figure 1). This physical stationary problem consists of studying the flow between two coaxial cylinders having an infinite length. The inner one with radius equal to a rotates around the common axis with an angular velocity V_τ/a and an axial velocity V_1. The outer one with a radius equal to b is fixed. In the computation, a region bounded by the planes $z = 0$ and $z = 1$ was taken.

Taking $a = 1$ and $b = e$, the velocity and the pressure are expressed for $f = (0, 0, 0)$ by:

$$u(x, y, z) = (u_x, u_y, u_z),$$

with

$$u_x(x, y, z) = -y\left(\frac{V_\tau}{e^2-1}\frac{e^2-r^2}{r^2}\right),$$

$$u_y(x, y, z) = x\left(\frac{V_\tau}{e^2-1}\frac{e^2-r^2}{r^2}\right),$$

$$u_z(x, y, z) = V_1(1-\ln r)$$

and

$$p(x, y, z) = \frac{V_\tau^2}{(e^2-1)^2}\left[\frac{r^2}{2} - \frac{e^4}{2r^2} + 2e^2(1-\ln r)\right].$$

The boundary conditions are:

- $u = 0$ on the outer cylinder,
- u equals the velocity prescribed as above on the inner cylinder,
- $\partial u/\partial z = 0$ on the two faces given by $z = 0$ and $z = 1$.

The pressure is set to vanish at a given point of the outer cylinder. The computations were performed by meshing one quarter of the domain using two orthogonal symmetry planes intersecting at axis $(0, z)$, thereby generating again 1331 nodes.

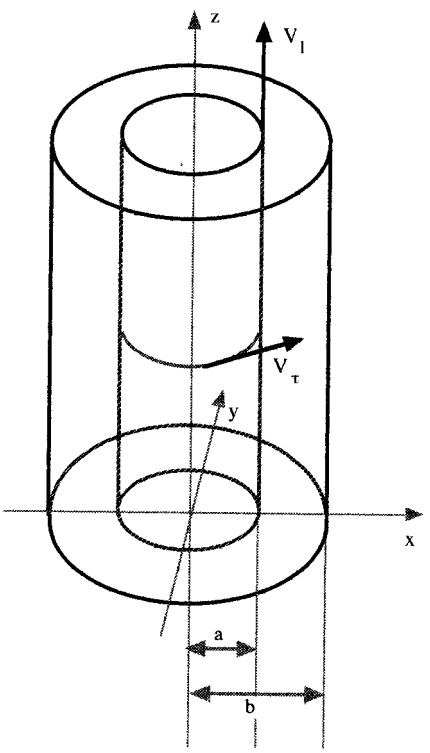

Figure 1. Modified Couette flow.

Here, neither of the two Goda algorithms led to the stationary solution. This is rather upsetting since the tests were performed with $Re = 10$.

Nevertheless, this experiment allowed the conclusion of the great robustness of the Chorin–Temam algorithm for stationary problems, for which the Goda one appears to be more uncertain. However, when the exact solution could be reached, the latter produced more accurate results. Here again, the fact that the condition $\partial p/\partial n = 0$ does not hold in both test problems above could explain the observed convergence defaults. Moreover, the quality of the pressure results obtained through the post-processing clearly justifies the use of this technique.

Remark 2: The convergence of the algorithm is checked on the basis of the maximum norm of the velocity increment between two time steps. Notice that the corresponding pressure increment may not converge within a prescribed tolerance even if the velocity increment does. This should not be surprising since the pressure approximation properties are known to be poorer than the velocity ones for projection algorithms. Moreover, the more severe convergence defaults observed for the Couette problem might have been enhanced by the prescribed Neumann velocity boundary condition on both ends of the corresponding computational domain.

6.2. Results in the non-stationary model problem

The computational results reported here and compared with experimental data correspond to the very early stages of the flow past a cylinder, during which the existence of two symmetry planes is observed.

First reported are the results related to the study of the different outflow boundary conditions with the original Chorin–Temam algorithm. In this part, a mesh denoted by Mesh 1, consisting of 8723 nodal points, namely the vertices of 44352 tetrahedrons, is used. The different parameters are $Re = 200$, $\rho = 0.05$ and $\Delta t = 0.05$. The shortest length of the cylinder is considered.

Since the boundary conditions for all the components of u_* are identical in the case of the conditions C.L. 2 and C.L. 3, in their implementation the authors did not use any penalty technique of a Dirichlet boundary condition applied to one or two of these components, like in the case of C.L. 1, C.L. 4 and C.L. 5. This procedure is necessary in the latter cases, in order to allow the use of only one sparse matrix data structure for the three components, although the iterative solution itself is not identical for all of them like in the case of C.L. 2 and C.L. 3. For this reason, the latter have an *a priori* advantage over the other boundary conditions considered in this work.

In all the cases a fairly good approximation of the flow is obtained right after the cylinder. The best results are given by C.L. 1 and C.L. 5, whereas C.L. 2 and C.L. 4 do not respect the physics of the problem very well. The worst results are those of C.L. 3. It can be observed in Figure 2 that the projections of the velocity field on the medium planes $z = 25$ and $y = 0$ at section $x = 10$ for the five conditions. Incidentally C.L. 1 yields an acceptable compromise between accuracy and computational cost. On the other hand, the post-processing does lead to a physically reasonable pressure field (Figure 3) both for C.L 1 and C.L. 5 (for C.L. 5 the pressure is prescribed to be zero at point $(-1.0, 0.0, 2.5)$).

Clearly, further studies are necessary on such topics, which still deserve much of specialists' attention. Nevertheless, the authors experiments allowed the ruling out of some out-

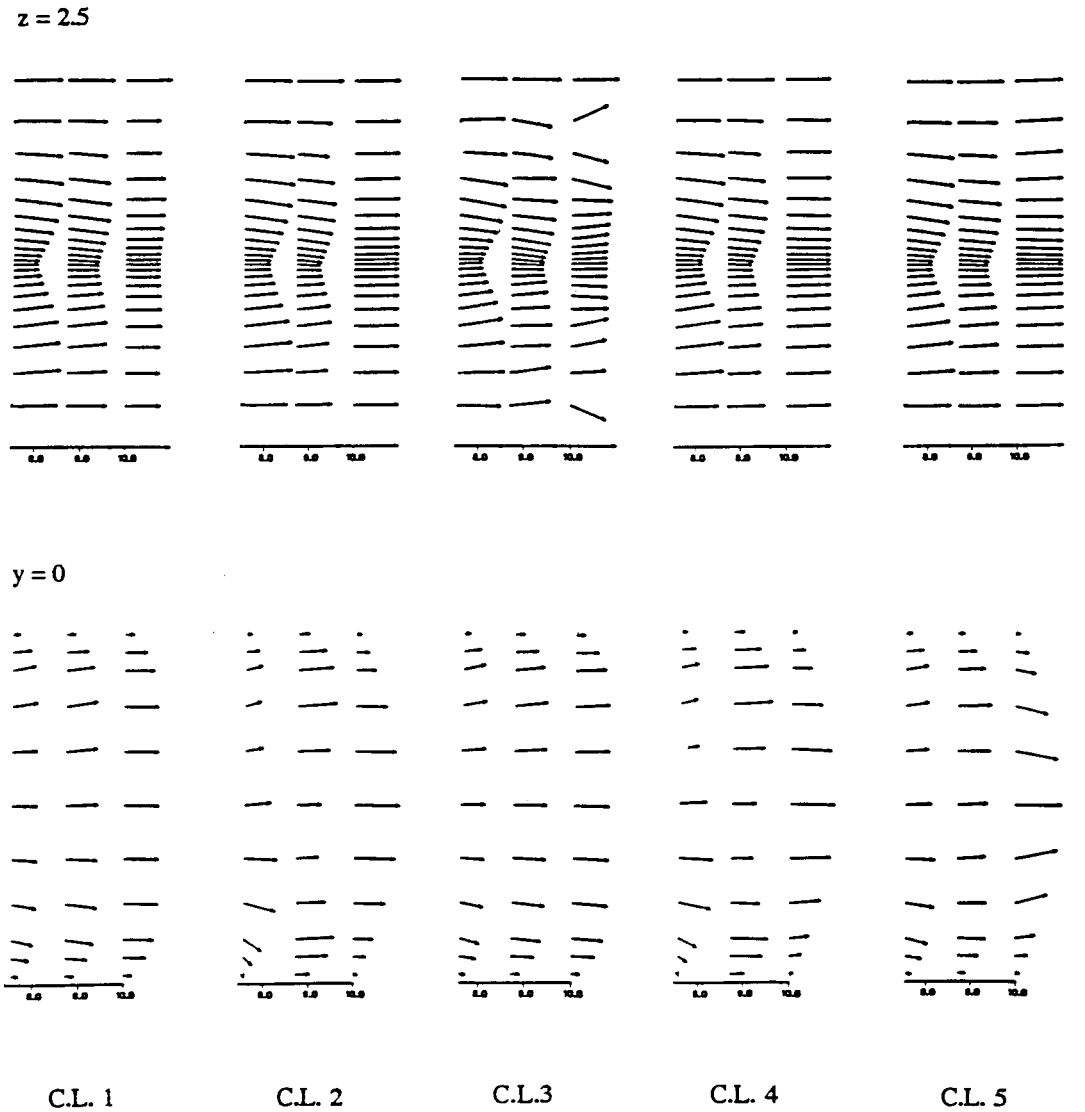

Figure 2. Velocity projections on planes $z = 2.5$ and $y = 0$ near the outflow boundary at time $t = 13$ for $Re = 200$ computed with boundary conditions C.L. 1–5, the original Chorin–Temam algorithm and Mesh 1.

flow boundary conditions that might seem attractive in the context of projection algorithms. Moreover, they encourage the use of some others as more likely to yield realistic results, while being rather easy to implement. In this respect, the authors hope to have given an useful contribution to all those who face the difficult choice of outflow boundary conditions for external flows.

In the second part of this study, they consider a flow at a higher Reynods number equal to 1000 past the longest cylinder. The mesh now denoted by Mesh 2 consists of 34947 nodal points corresponding to 190848 tetrahedrons, but symmetry of the flow with respect to the planes $y = 0$ and $z = 5$ has been assumed. The numerical parameters are $\rho = 0.025$ and $\Delta t = 0.05$. The selected outflow boundary condition is C.L. 1 taking into account the former results.

The three types of schemes have been implemented: the Chorin–Temam, the Goda and the modification of the latter in which one does not perform the Petrov–Galerkin stabilization on the pressure term of (9). Like in the stationary cases, irregularities were observed with the first

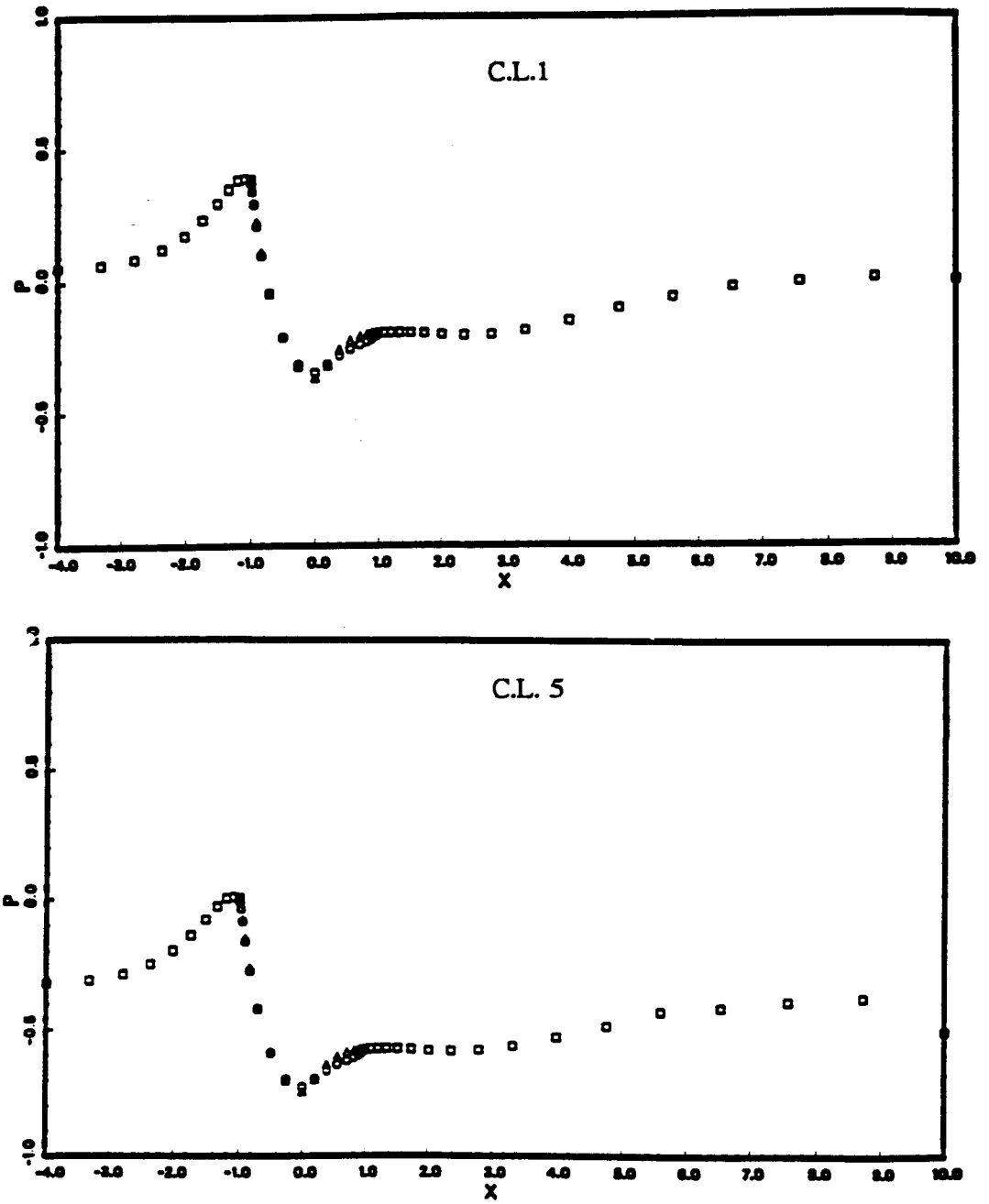

Figure 3. Pressure profile along the x-axis and on the cylinder for $z = 2.5$ at time $t = 13$ for $Re = 200$ computed with boundary conditions C.L. 1 and C.L. 5, the original Chorin–Temam algorithm and Mesh 1.

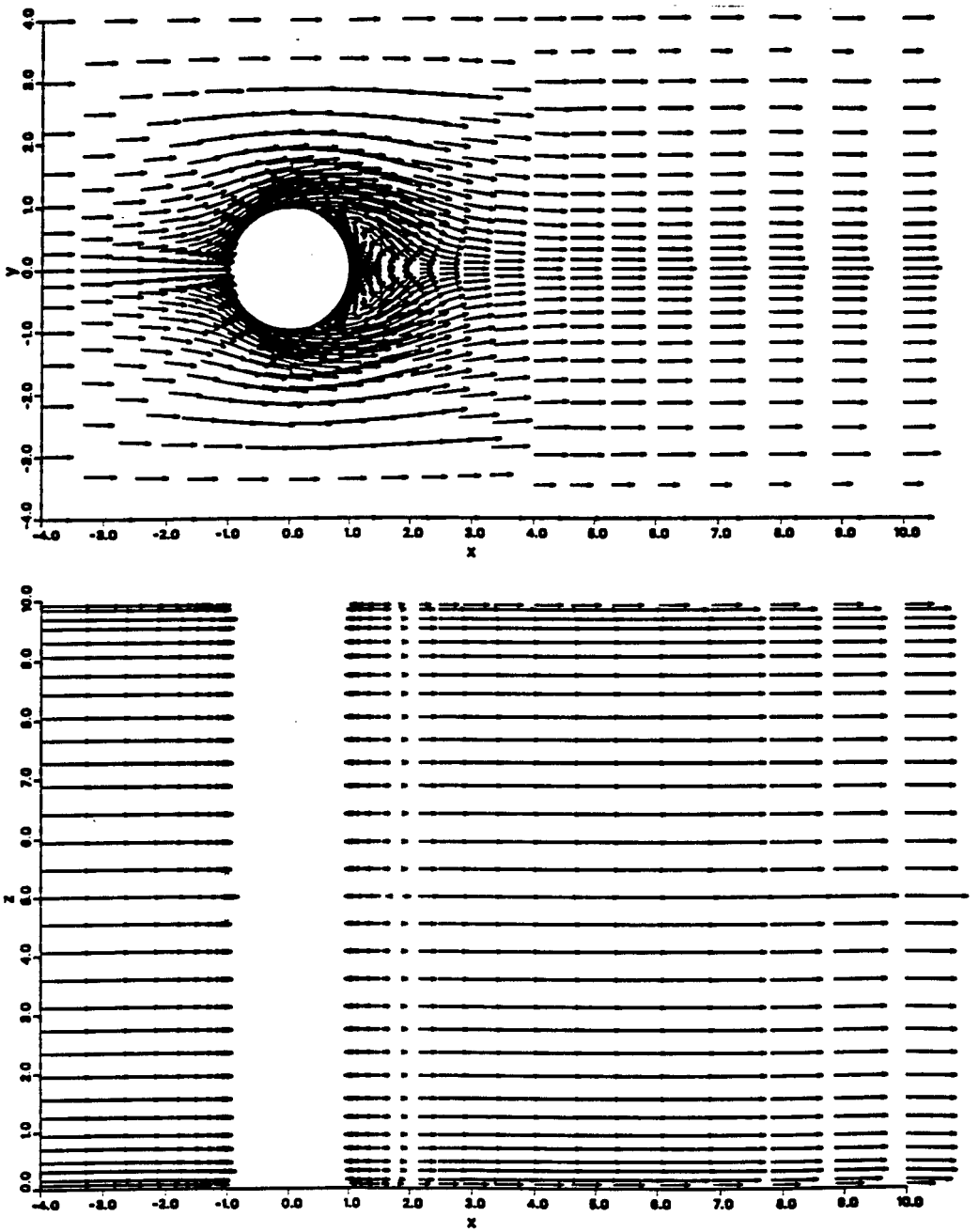

Figure 4. Original Chorin–Temam algorithm (Mesh 2). Projections of the velocity field on planes $z = 5$ and $y = 0$ at time $t = 2$ for $Re = 1000$ and boundary condition C.L. 1.

algorithm probably due to the poorer accuracy of this projection method (Figure 4). On the other hand, a considerably better behavior was attained with the second version of Goda's algorithm. Figure 5 shows a view of the velocity field at $t = 2.0$ on planes $y = 0$ and $z = 5$, obtained with the very same algorithm.

Finally, with a finer mesh denoted by Mesh 3 with 65403 nodal points corresponding to 364392 tetrahedrons, a realistic simulation of the flow as it evolves in time was observed (Figures 6–9).

Furthermore, note that this configuration allows comparisons with other works, both numerical and experimental. The top of Figures 10 and 11 shows a zoom near the cylinder of

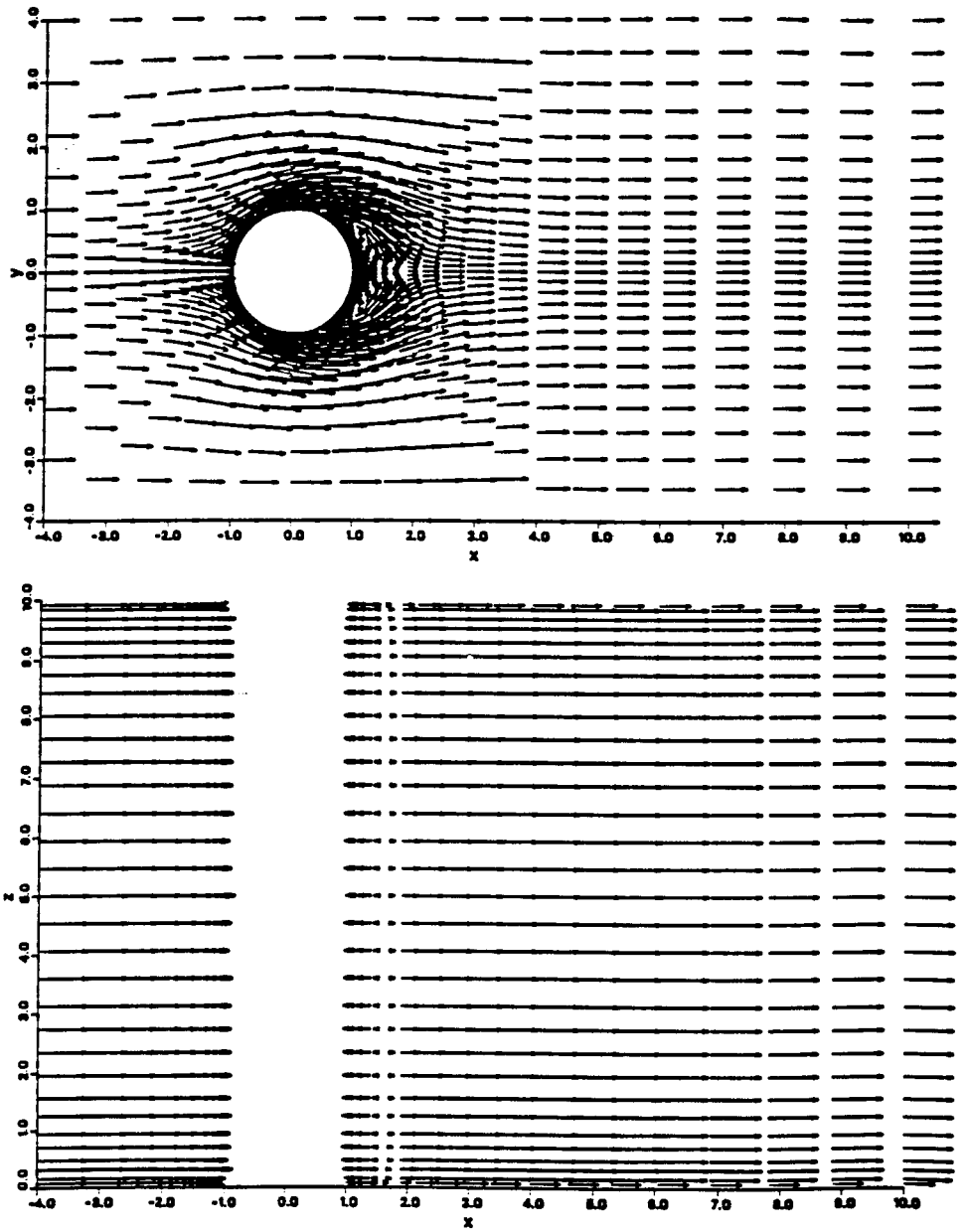

Figure 5. Modified Goda algorithm (Mesh 2). Projections of the velocity field on planes $z = 5$ and $y = 0$ at time $t = 2$ for $Re = 1000$ and boundary condition C.L. 1.

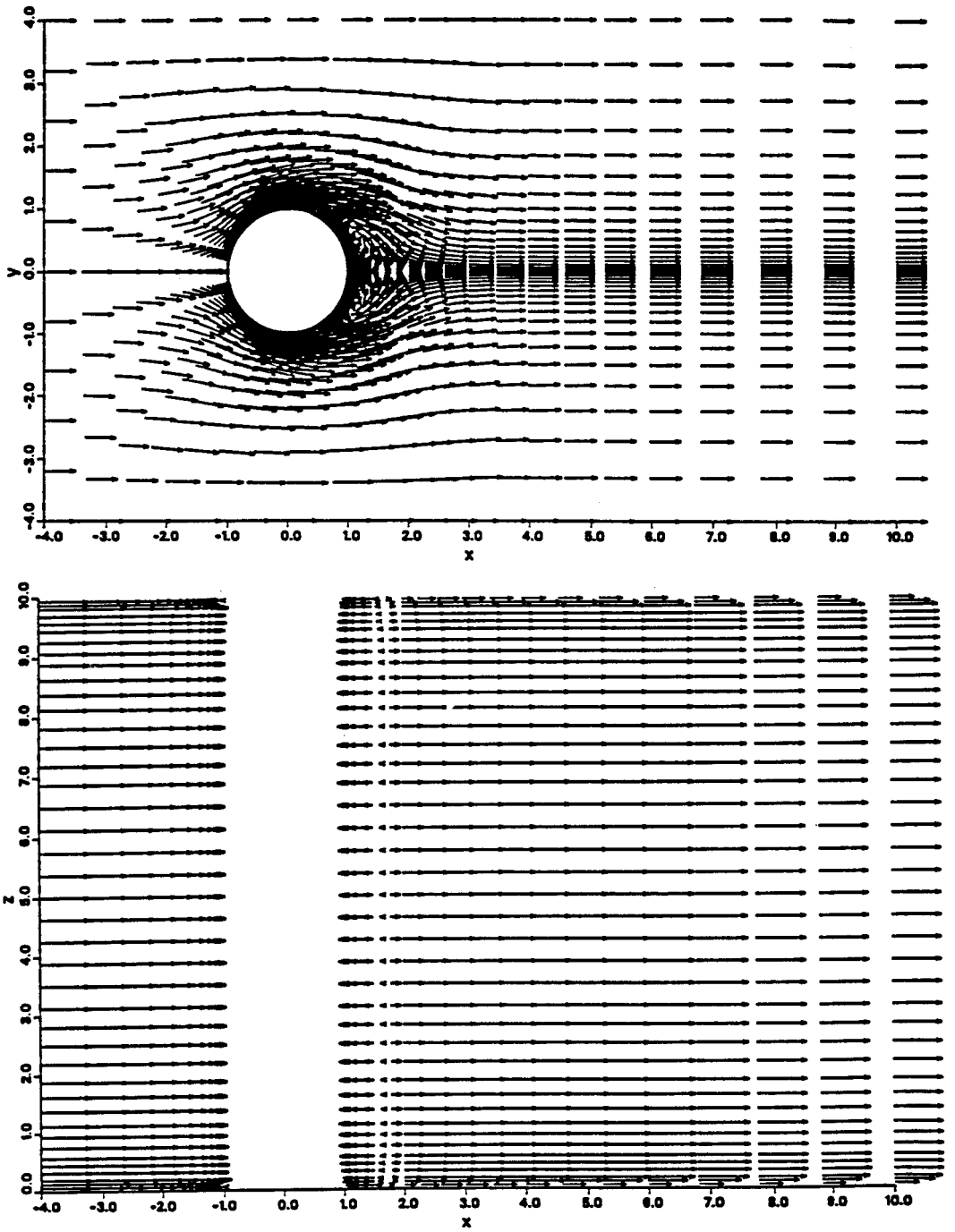

Figure 6. Modified Goda algorithm (Mesh 3). Projections of the velocity field on planes $z = 5$ and $y = 0$ at time $t = 2$ for $Re = 1000$ and boundary condition C.L. 1.

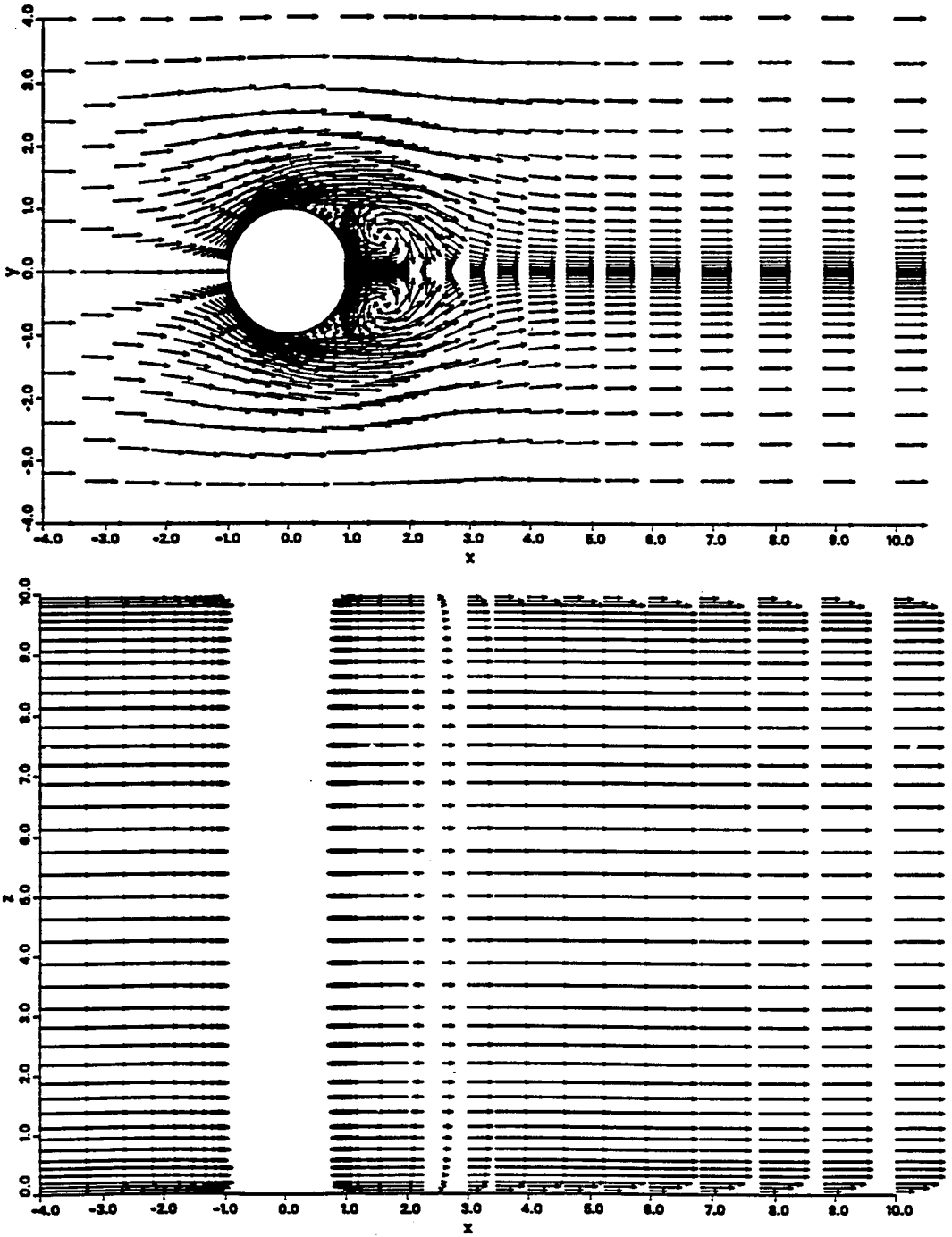

Figure 7. Modified Goda algorithm (Mesh 3). Projections of the velocity field on planes $z = 5$ and $y = 0$ at time $t = 4$ for $Re = 1000$ and boundary condition C.L. 1.

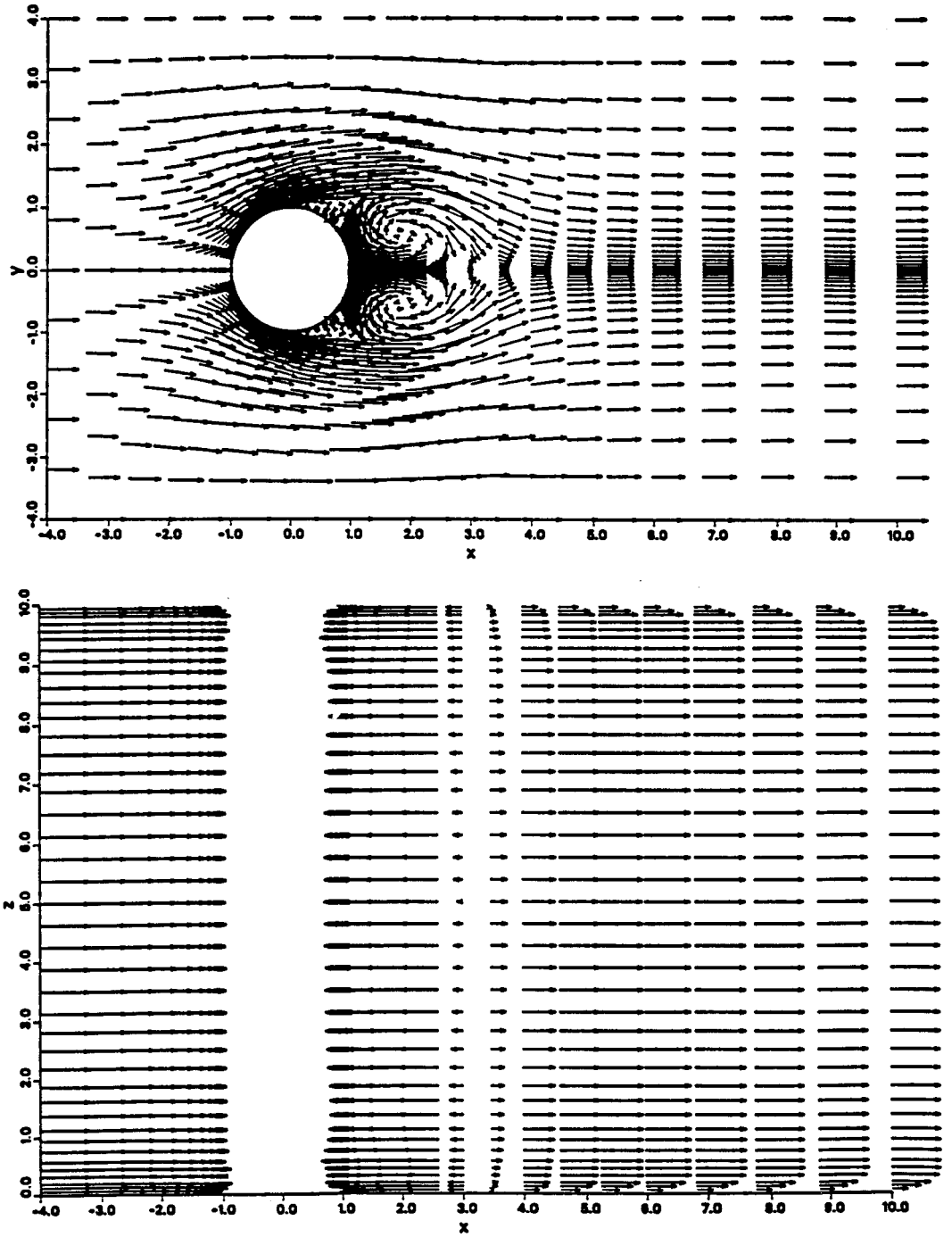

Figure 8. Modified Goda algorithm (Mesh 3). Projections of the velocity field on planes $z = 5$ and $y = 0$ at time $t = 6$ for $Re = 1000$ and boundary condition C.L. 1.

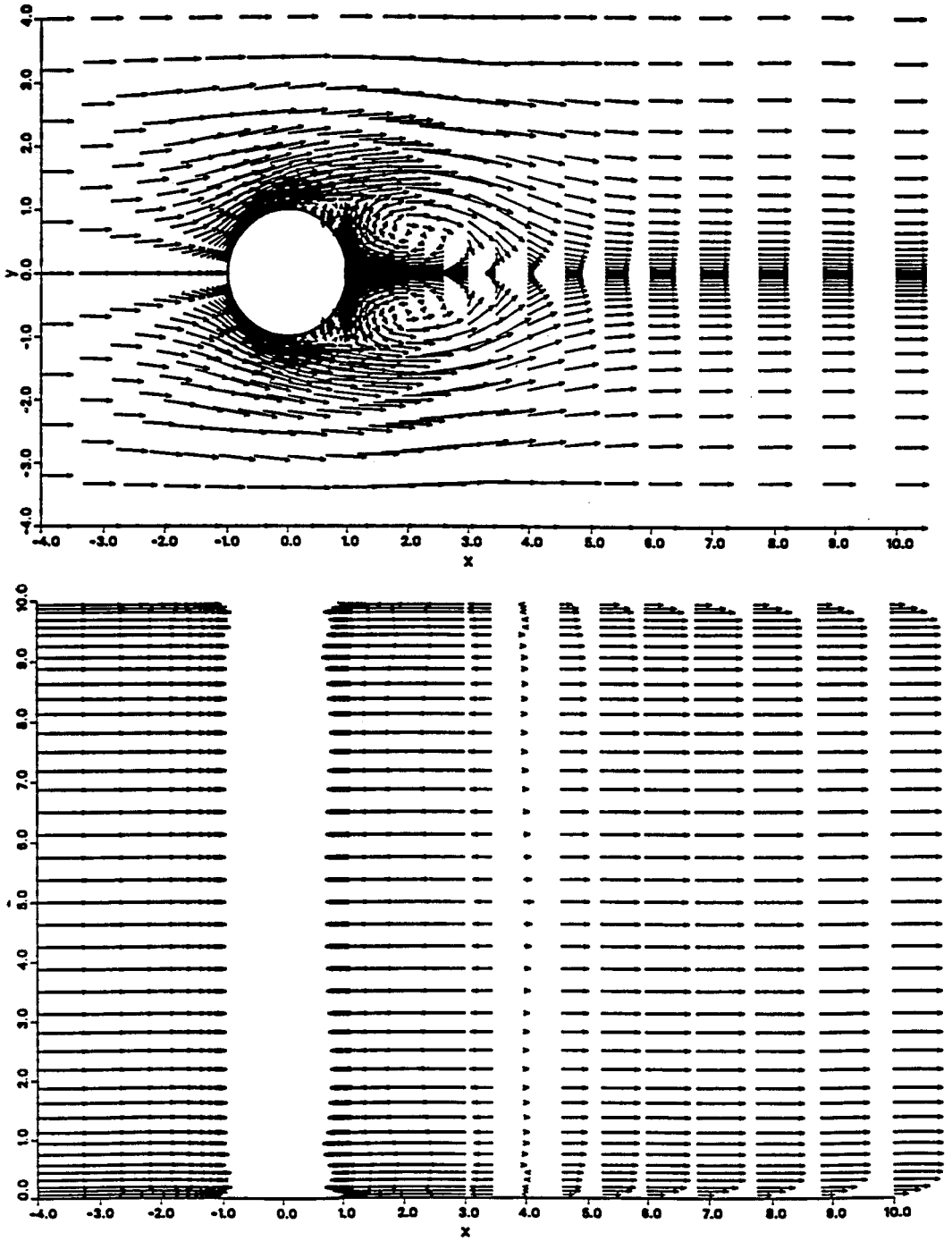

Figure 9. Modified Goda algorithm (Mesh 3). Projections of the velocity field on planes $z = 5$ and $y = 0$ at time $t = 8$ for $Re = 1000$ and boundary condition C.L. 1.

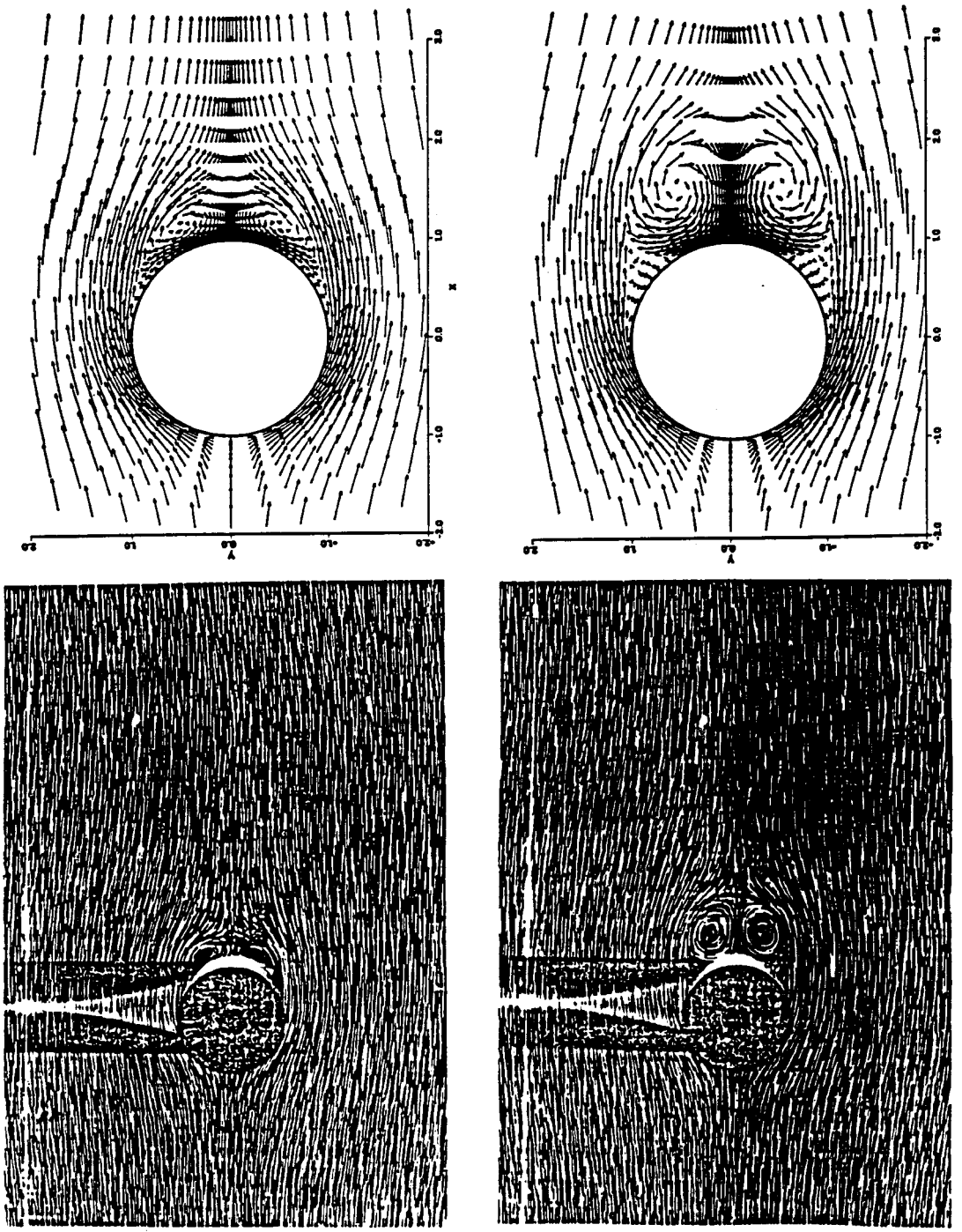

Figure 10. Modified Goda algorithm (Mesh 3). A comparison of numerical results near the cylinder with experimental data for $Re = 1000$ at times $t = 2$ and $t = 4$.

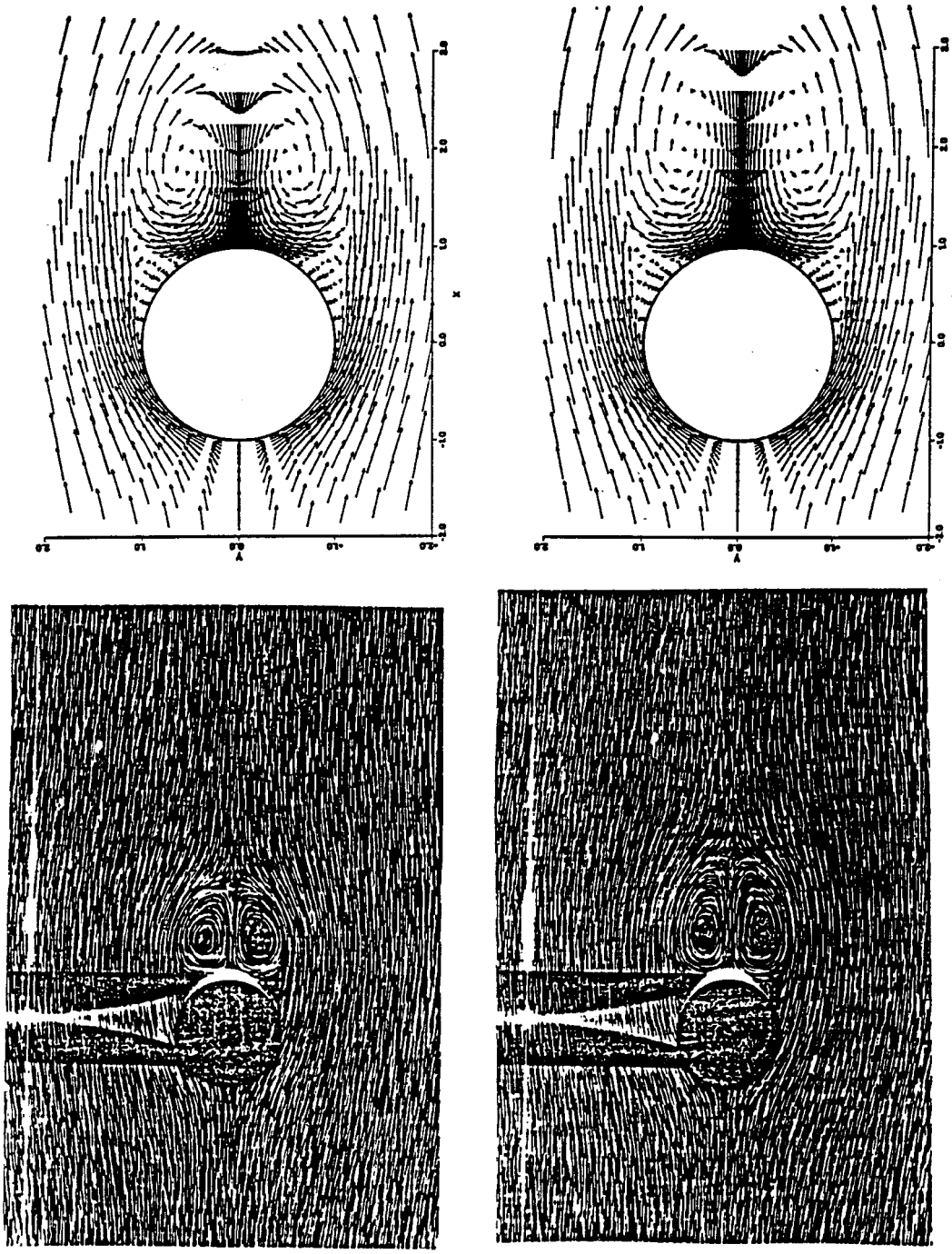

Figure 11. Modified Goda algorithm (Mesh 3). A comparison of numerical results near the cylinder with experimental data for $Re = 1000$ at times $t = 6$ and $t = 8$.

the velocity field on plane $z = 5$ for $t = 2.0–8.0$. At the bottom, images of the same fields processed with an experimental arrangement performed by Coutenceau *et al*. [20] are shown.

Further details about the whole numerical scheme and other computer results mainly obtained on the Cray C98 of IDRIS, CNRS, France, can be found in [18].

Remark 3: For a realistic simulation of the flow past a cylinder at later stages, the two symmetry assumptions made here would have to be dropped.

7. CONCLUSIONS

In this paper the authors have shown through a number of examples that classical linear finite elements represent a convenient choice to approximate both velocity and pressure in the framework of the solution of the Navier–Stokes equations by projection methods, provided a post-processing of the latter field using the former one is performed. Among the three versions of the algorithm tested here, the Chorin–Temam one seems to be more reliable to treat stationary problems, although the so-called modified Goda algorithm showed globally a better accuracy in all the cases.

In any case, projection algorithms may show a poor performance when used to solve stationary problems. The assertion could be explained by the systematic prescription of a homogeneous Neumann boundary condition to the pressure determined through standard versions of such algorithms. For this reason too, the computation of a post-processed pressure may remedy this drawback to some extent, as one can clearly infer from the solution of the modified Couette flow test problem.

Checking the efficiency of different types of outflow boundary conditions to be implemented in connection with the splitting that characterizes projection algorithms was one of the purposes of this paper. It has been found that easy to implement outflow boundary condition CL. 1 in the context of such numerical approaches combined with the finite element method, produces physically acceptable results for relatively short computational domains past an obstacle in external flow simulation.

Finally, as an important conclusion in the light of the experiments performed in this paper, the authors recommend the modified Goda algorithm with pressure post-processing by a sort of least-squares methods as a reliable methodology to solve the time-dependent Navier–Stokes equations. Moreover, the SUPG stabilization (which incidentally is strictly linked with such modifications of the original Goda's algorithm) turns out to be a powerful tool to allow the use of different versions of the pre-conditioned conjugate gradient method, to solve non-symmetric discretized advection–diffusion matrix systems.

Summarizing, the authors attempted to clarify the issue concerning the performance that can be actually expected from projection methods in the computer solution of real life flow problems. In view of the above conclusions and taking into account the present state of the art as far as three-dimensional viscous incompressible flow is concerned, they do hope that their work brings about a constructive contribution to this field.

REFERENCES

1. M.O. Bristeau, O. Pironneau, R. Glowinski, J. Periaux and P. Perrier, 'On the numerical solution of non linear problems in fluid dynamics by least squares and finite element methods (I) Least square formulation and conjugate gradient solution of the continuous problems', *Comput. Methods Appl. Mech. Eng.*, **17/18**, 619–657 (1979).

2. R. Glowinski, 'Fictitious domain/domain decomposition method for viscous flow calculation', *Mafelap 1996* (*Conference on the Mathematics of Finite Element and Applications*), Brunel University ED, 1996, p. 47.
3. M. Shimura and M. Kawahara, 'A new approach for pressure boundary condition using the velocity correction method', in Niki and Kawahara (eds.), *Computational Methods in Flow Analysis*, vol. 18, Okayama University of Science, 1988, pp. 446–453.
4. J.G. Heywood, R. Rannacher and S. Turek, 'Artificial boundaries and flux and pressure conditions for the incompressible Navier–Stokes equations', *Int. J. Numer. Methods Fluids*, **22**, 325–352 (1996).
5. V. Ruas, 'Finite element methods for three incompressible viscous flow', *Finite Elem. Fluids*, **8**, 211–235 (1992).
6. V. Ruas, L. Quartapelle and J. Zhu, 'A symmetrized velocity–vorticity formulation of three-dimensional Stokes system', *C. R. Acad. Sci Paris*, **323**, 819–824 (1996).
7. A. Chorin, 'Numerical simulation of the Navier–Stokes equations', *Math. Comput.*, **22**, 745–762 (1968).
8. R. Temam, 'Une méthode d'approximation de la solution des équations de Navier–Stokes', *Bull. Soc. Math. France*, **98**, 115–152 (1968).
9. K. Goda, 'A multistep technique with implicit difference schemes for calculating two- or three-dimensional cavity flows', *J. Comput. Phys.*, **30**, 76–95 (1979).
10. A.N. Brooks and T.J.R. Hughes, 'Streamline-upwind/Petrov–Galerkin formulations for convection dominated flows with particular emphasis of the incompressible Navier–Stokes equations', *Comput. Methods Appl. Mech. Eng.*, **32**, 199–259 (1982).
11. H.A. Van Der Vorst, 'Bi-CGSTAB: a fast and smoothly converging variant of Bi-CG for the solution of non-symmetric linear systems', *SIAM J. Sci. Stat. Comput.*, **13**, 631–644 (1992).
12. R.L. Sam and P.M. Gresho, 'Résumé and remarks on the open boundary condition minisymposium', *Int. J. Numer. Methods Fluids*, **18**, 983–1008 (1994).
13. L.P. Franca and S.L. Frey, 'Stabilized finite element methods: II. The incompressible Navier–Stokes equations', *Comput. Methods Appl. Mech. Eng.*, **99**, 209–233 (1992).
14. M.A. Behr, L.P. Franca and T.E. Tezduyar, 'Stabilized finite clement methods for the velocity–pressure–stress formulation of incompressible flows', *Comput. Methods Appl. Mech. Eng.*, **104**, 3148 (1993).
15. L.P. Franca and T.J.R. Hughes, 'Convergence analyses of Galerkin least-squares methods for symmetric advective–diffusive forms of the Stokes and incompressible Navier–Stokes equations', *Comput. Methods Appl. Mech. Eng.*, **105**, 285–298 (1993).
16. T.E. Tezduyar, J. Liou, D.K. Ganjoo and M. Behr, 'Solution techniques for the vorticity–streamfunction formulation of two-dimensional unsteady incompressible flows', *Int. J. Numer. Methods Fluids*, **11**, 515–539 (1990).
17. T.E. Tezduyar, R. Glowinski and J. Liou, 'Petrov–Galerkin methods on multiply connected domains for the vorticity–streamfunction formulation of the incompressible Navier–Stokes equations', *Int. J. Numer. Methods Fluids*, **8**, 1269–1290 (1988).
18. D. Goldberg, 'Applications de la méthode des projections au calcul par éléments finis d'écoulements tridimensionnels de fluides visqueux incompressibles', *Thèse de Doctorat*, Université Pierre et Marie Curie, 1994.
19. J.L. Guermond and L. Quartapelle, 'On stability and convergence of projection methods based on pressure Poisson equation', *Int. J. Numer. Methods Fluids*, **26**, 1039–1053 (1998).
20. Ta Phuoc Loc, W. Labidi, A. Dulieu, M. Coutenceau, G. Pineau and A. Texier, 'Simulation numérique d'ecoulements instationnaires tridimensionnels par résolution des équations de Navier–Stokes sur un système multiprocesseur', *Rapport final de synthese de la convention DRET/LIMSI N°88/047*, 1990.

